Liquid-State Anomalies and the Stell-Hemmer Core-Softened Potential

M. Reza Sadr-Lahijany, Antonio Scala, Sergey V. Buldyrev, and H. Eugene Stanley
Center for Polymer Studies and Department of Physics, Boston University, Boston, Massachusetts 02215
(Received 15 May 1998; revised manuscript received 15 October 1998)

We study the liquid anomalies arising from the Stell-Hemmer interaction, using molecular dynamics simulations and approximate 2D solutions. We observe in the liquid phase three types of anomalies: (i) An increase in specific volume upon cooling, (ii) an increase in isothermal compressibility upon cooling, and (iii) an increase in the diffusion coefficient with pressure. We relate the anomalies to the existence of two different local structures in the liquid phase. [S0031-9007(98)07749-7]

PACS numbers: 61.20.Gy, 61.25.Em, 64.70.Ja, 65.70.+y

In their pioneering work, Stell and Hemmer proposed the possibility of a second critical point in addition to the normal liquid-gas critical point for potentials that have a region of negative curvature in their repulsive core (henceforth referred to as core-softened potentials) [1]. They also pointed out that for the 1D model with a long range attractive tail, the isobaric thermal expansion coefficient, $\alpha_P \equiv V^{-1}(\partial V/\partial T)_P$ (where V, T, and P are the volume, temperature, and pressure), can take an anomalous negative value. Debenedetti *et al.*, using thermodynamic arguments, noted that a "softened core" can lead to $\alpha_P < 0$ [2].

The issue of liquid anomalies by itself is an interesting phenomenon which is not limited to the density anomaly. In this Letter we also discuss two other types of liquid anomalies, increase of isothermal compressibility (density fluctuations) upon cooling, and increase of diffusion coefficient (decrease of viscosity) with pressure. These anomalies occur in many liquids [3,4], including liquid water [3,5]. *Ab initio* calculations [6] or inversion of structure factor data [6,7] reveal that a core-softened potential can be considered a realistic first order approximation for the interaction [7,8], even in the case of network forming anomalous liquids [3].

Previous works showed that a density anomaly derived in 1D does not necessarily hold in higher dimensions [9,10]. Here we demonstrate, by means of numerical simulations for $d = 2$, that the core-softened potential can lead to all three anomalies and that an explanation for the occurrence of these anomalies can be given in terms of the shape and parameters of the potential. To the best of our knowledge this is the first time that a simple radially symmetric potential is shown to yield these anomalies. We also revisit the question of the second critical point in relation with these anomalies.

The core-softened potential that we study is shown in Fig. 1(a). It is composed of a hard core of diameter a which has a repulsive shoulder of width $b - a$ and depth $\lambda\epsilon$, and an attractive well of width $c - b$ and depth ϵ [11].

We first study the system in 1D to get familiar with the possible properties that might arise in higher dimensions. We derive the exact form of partition function and equation of state, following the methods of [4,9,12,13]. The resulting isobars shown in Fig. 1(b) exhibit two different types of behavior depending on the pressure. Note that there is a discontinuity in ℓ, the average distance per particle, at an upper pressure $P = P_{\rm up}$ along the $T = 0$ isotherm. For all $P > P_{\rm up}$, $\ell = a$ at $T = 0$, and ℓ increases monotonically with T. For $P < P_{\rm up}$, $\ell = b$ at $T = 0$, and the $\ell(T)$ isobars show a maximum and a minimum, which correspond, respectively, to points of minimum and maximum density [4,9,14].

We also study the isothermal compressibility $K_T \equiv -V^{-1}(\partial V/\partial P)_{T,N}$. Figure 1(c) shows an anomalous region along isobars in which K_T increases upon cooling. We find that the maximum value of K_T grows as $P \to P_{\rm up}$, and K_T diverges as $1/T$ when we approach

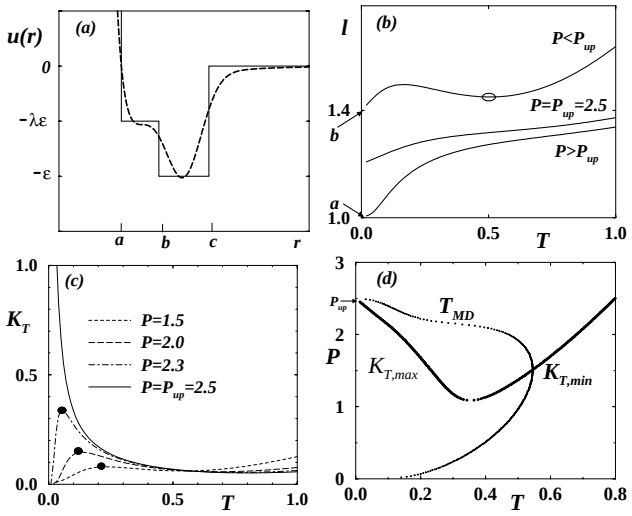

FIG. 1. (a) General form for the core-softened potential studied here. The length parameters a, b, c and energy parameters ϵ, λ are shown. The dashed curve is the smooth version [11]. (b) Isobars of ℓ, the average distance per particle, for the discrete 1D core-softened potential [11] with $P_{\rm up} = 2.5$ in agreement with Eq. (1). The $T_{\rm MD}$ point is marked by an open circle. (c) Isothermal compressibility for the discrete potential along different isobars, with their maxima marked by filled circles. K_T along $P_{\rm up}$ isobar diverges as $1/T$. (d) The loci of $T_{\rm MD}$ and K_T extrema for the discrete potential.

the point C' with coordinates $(T = 0, P = P_{up})$ which we interpret as a critical point [15]. Further, the locus of K_T extrema joins the point C' [Fig. 1(d)]. We also note that the locus of K_T extrema intersects the temperature of maximum density (T_{MD}) locus at its infinite slope point, a result that is thermodynamically required [16]. Such a point on the T_{MD} line has been observed in simulations which support the existence of a second critical point in supercooled water [17].

Next we consider whether the anomalies derived for $d = 1$ hold for $d > 1$ [10]. To this end, we perform molecular dynamics (MD) simulations for a 2D system composed of N disks in a rectangular box. For the discrete version of the potential, we use the collision table technique [18] for $N = 896$ disks, and for the smooth version of the potential, we use the velocity Verlet integrator method [18] for $N = 2500$ disks [19]. Figure 2 shows the results derived for the smooth version. Our MD results are qualitatively similar for the discrete and smooth versions. Figure 2(a) shows P versus T along liquid isochores (constant ρ) which terminate at the freezing line. We identify the freezing line as the locus of the points where the diffusion coefficient vanishes and the system acquires the structure of a 2D solid [20]. For $P < P_0 \sim 1$, where the freezing line has a negative slope, the liquid has a T_{MD} characterized by a minimum along the isochore [21], and it freezes into a solid with a lower density than the liquid [22]. This solid has a triangular lattice structure with a lattice constant b. For $P > P_0$, the liquid T_{MD} vanishes, the solid is denser than the liquid, and it has a square lattice structure with lattice constant a. Near the freezing line, the liquid acquires a local structure similar to the nearby solid.

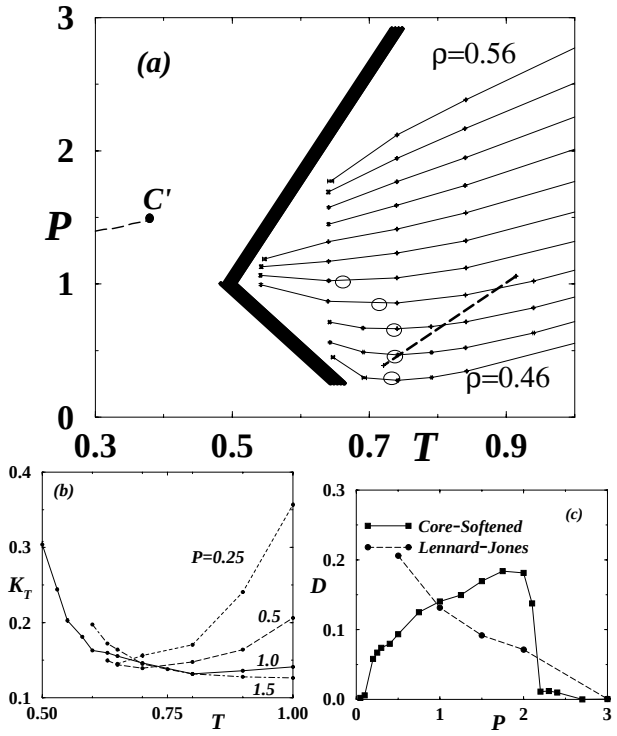

FIG. 2. MD results for the smooth potential with the same parameters as in Fig. 1(a) [11]. (a) Constant density curves with, from bottom to top, densities between 0.46 to 0.56 in steps of 0.01. The open circles mark T_{MD}, and the dashed line crossing the T_{MD} line is the locus of K_T minima from (b). The thick gray line is the approximate loci of the freezing points, and the dashed line ending at the critical point C' is the LDL to HDL transition line derived from the cell theory approximation. (b) Isothermal compressibility along isobars. Except for the $P = 0.25$ isobar, the graphs show anomalous increase upon cooling. (c) Diffusion coefficient D (slope of the mean square displacement as a function of time) for different pressures at $T = 0.65$, showing an anomalous increase in the $P < 1.7$ range. For comparison, we show $D/4$ for a Lennard-Jones liquid at $T = 0.7$, from simulation of 2304 disks. The zero values at low pressure for the core softened and at high pressures for both correspond to a solid phase.

The three anomalies can be related to the interplay between two local structures, an open structure in which the nearest neighbor particles are typically at a distance b, and a denser structure in which the nearest neighbors penetrate into the softened core and are typically at a smaller distance a. The configurations are determined by the minima of the Gibbs potential, $G(T, P) = U + PV - TS$ (where G, U, and S are the Gibbs potential, internal energy, and entropy). Figure 3(a) shows G for 1D at $T = 0$ for two different values of P. The qualitative shape should not change for higher d. For low pressures at small T, the open structure is favored by the Gibbs potential. Increasing T for these pressures will increase local fluctuations in the form of dense structures which can lead to an overall contraction of the system upon heating, causing a density anomaly. Increasing P, on the other hand, raises the relative free energy of the open structure, until the dense structure will be the favored local structure, as seen for $P > P_{up}$ in Fig. 3(a).

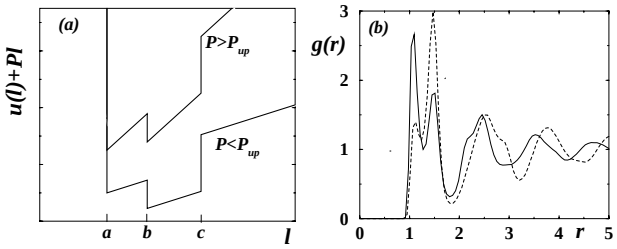

FIG. 3. (a) The 1D Gibbs potential at $T = 0$ as a function of the extra "degree of freedom" ℓ, for the discrete form of potential in Fig. 1(a). The equilibrium value of $\ell(P)$ is determined as the absolute minimum of this function, which is located at $\ell = b$ below P_{up} and at $\ell = a$ above P_{up}. (b) First few peaks of $g(r)$ for $P = 0.5$ (dashed line) and $P = 2.0$ (solid line) on the $T = 0.65$ isotherm which was used in Fig. 2(c). The changes in the first (split) peak indicate that increasing P lowers the total number of particles in the open structure ($r \approx 1.5$) and increases the number of particles in the dense structure ($r \approx 1.1$).

At small T this pressure dependence can lead to a first order transition, while for large T the transition is smooth. At $T = 0$, the value of P_{up} is found by equating Gibbs potentials,

$$P_{\text{up}} = -(U_{\text{open}} - U_{\text{dense}})/(V_{\text{open}} - V_{\text{dense}}). \quad (1)$$

For the discrete potential of Fig. 1(a), we find $P_{\text{up}} = (1 - \lambda)\epsilon/(b - a)$ in 1D, in agreement with the value of P_{up} derived from the 1D equation of state [Fig. 1(b)] [9]. In higher d, Eq. (1) helps to estimate the pressure region in which we expect an overall shift from one local structure to another.

We investigate the compressibility anomaly by measuring K_T for each state point [23] and plotting it along isobars as in Fig. 2(b). We observe that along some isobars K_T increases upon cooling. As in 1D, the locus of K_T extrema intersects the T_{MD} line at its infinite slope point [Fig. 2(a)], which is consistent with thermodynamic arguments [16]. If the increase in K_T is due to the existence of a critical point C' on the liquid free energy surface (like in 1D), then by fitting the K_T curve to a power law divergence we can estimate the location of C' to be in the region $0.3 < T < 0.5$ and $1.0 < P < 1.5$. C' is inside the solid phase region, and is not accessible to the liquid in our MD method.

In order to investigate the possibility of C', we perform a 2D cell theory estimate of the equation of state using a method similar to the original spherical Lennard-Jones and Devonshire cell theory method [24]. This method assumes that each particle is confined to a circular cell, whose radius is determined by the average area per particle, v. The cell theory method neglects the correlation between the positions of different particles and assumes that the potential acting on each particle is a result of interacting with all its nearest neighbors smeared around its cell. The Helmholtz potential per cell is

$$h(v, T) = h_{\text{id}}(v, T) - k_B T \ln[v_{\text{eff}}(v, T)/v], \quad (2)$$

where $h_{\text{id}}(v, T)$ is the ideal gas Helmholtz potential and the effective volume of a cell is defined as

$$v_{\text{eff}}(v, T) \equiv \int_{\text{cell}} e^{-\beta u(x)}\, d\mathbf{x} \quad (3)$$

with the core-softened potential used for $u(\mathbf{x})$. For each state point (P, T), we find the value of v by minimizing $h(v, T) - Pv$. The resulting phase diagram has two lines of first order phase transition, a low pressure line which is the liquid-gas phase transition line terminating at a critical point C, and a high pressure line that separates a low-density liquid (LDL) and a high-density liquid (HDL) and terminates in a critical point C' [Fig. 2(a)]. The location of C' agrees with our previous estimate from K_T.

We next study the diffusion anomaly using our MD results. We measure the diffusion coefficient D from the slope of the mean square displacement as a function of time. In analogy with the case of liquid water [5], along low T liquid isotherms increasing P increases D [Fig. 2(c)]. We explain this anomaly by noting that D is proportional to the mean free path of particles. The mean free path increases with free volume per particle $v_{\text{free}} \equiv v - v_{\text{ex}}$, where v_{ex} is the excluded volume per particle resulting from the effective hard core. Note that for the dense structure $v_{\text{ex}} \propto a^2$ which is smaller than $v_{\text{ex}} \propto b^2$ for the open structure. Increasing P decreases v but can also decrease v_{ex} by transforming some of local open structures to dense structures. Since both v and v_{ex} decrease with P and since $\Delta v_{\text{free}} = \Delta v - \Delta v_{\text{ex}}$, the effect of P on D depends on whether Δv or Δv_{ex} dominates. The anomalous increase in D along the isotherms near the freezing line is a sign of the dominance of the Δv_{ex} term. Thus the anomaly in D must disappear near a certain pressure above which the average distance between particles corresponds to the dense structure and as a result the contribution of the open structure to v_{ex} is negligible [25].

To examine the transition from the open to the dense structure, we study the pair distribution function $g(r)$ for configurations corresponding to different state points [Fig. 3(b)]. We observe a uniform value of $g(r) \approx 1$ at large r which confirms that all the state points shown in Fig. 2(a) are in the liquid state. For small r the liquid shows a few peaks corresponding to the local structure in the liquid. The first peak in $g(r)$ splits into two subpeaks, which correspond to the locations of the nearest neighbors in the dense and open structures. The open structure subpeak decreases with P, while the dense structure subpeak increases. We observe the same change with T along liquid isobars. These observations agree with our previous arguments about the effect of P and T on the relative occurrence of the two types of structure.

In summary, we have found that a core-softened interaction can generate the three types of liquid anomalies studied in this work. We have also found that all three anomalies are related to the existence of two general types of local structures.

We thank D. Wolf for essential discussions, M. Canpolat, S. Harrington, S. Havlin, B. Urbanc, M. Meyer, S. Sastry, A. Skibinsky, F. W. Starr, and G. Stell for helpful suggestions and NSF for support.

[1] P. C. Hemmer and G. Stell, Phys. Rev. Lett. **24**, 1284 (1970); G. Stell and P. C. Hemmer, J. Chem. Phys. **56**, 4274 (1972); J. M. Kincaid, G. Stell, and C. K. Hall, *ibid.* **65**, 2161 (1976); J. M. Kincaid, G. Stell, and E. Goldmark, *ibid.*, **65**, 2172 (1976).

[2] P. G. Debenedetti *et al.*, J. Phys. Chem. **95**, 4540 (1991).

[3] P. G. Debenedetti, *Metastable Liquids* (Princeton University Press, Princeton, NJ, 1996); see also the very recent review O. Mishima and H. E. Stanley, Nature (London) (to be published).

[4] Y. Yoshimura, Ber. Bunsen-Ges. Phys. Chem. **95**, 135 (1991).

[5] F. T. Worrell, Nature (London) **207**, 620 (1965).

[6] K. K. Mon, N. W. Ashcroft, and G. V. Chester, Phys. Rev. B **19**, 5103 (1979); I. Yokoyama and S. Ono, J. Phys. F **15**, 1215 (1985); K. Hoshino *et al.*, J. Phys. F **17**, 787 (1987).
[7] T. Head-Gordon and F. H. Stillinger, J. Chem. Phys. **98**, 3313 (1993).
[8] D. A. Young, J. Chem. Phys. **58**, 1647 (1973).
[9] C. H. Cho *et al.*, Phys. Rev. Lett. **76**, 1651 (1996).
[10] E. Velasco *et al.*, Phys. Rev. Lett. **79**, 179 (1997).
[11] The smooth version of the potential resembles the discrete form and has the functional form $u(r) = 4\lambda'\epsilon'(r^{-12} - r^{-6}) - \epsilon' \exp\{-[w(r - r_0)]^n\}$. All of the results reported here are for the discrete potential with $a = 1$, $b = 1.4$, $c = 1.7$, $\epsilon = 2$, and $\lambda = 0.5$ and its smooth version with $\epsilon' = 1.7$, $\lambda' = 1/1.7$, $w = 5$, $r_0 = 1.5$, and $n = 2$ as shown in Fig. 1(a).
[12] H. Takahashi, Proc. Phys. Math. Soc. Jpn. **24**, 60 (1942); *Mathematical Physics in One Dimension*, edited by E. H. Lieb and D. C. Mattis (Academic, New York, 1966), pp. 25–34.
[13] A. Ben-Naim, *Statistical Thermodynamics for Chemists and Biochemists* (Plenum, New York, 1992).
[14] G. M. Bell and H. Sallouta, Mol. Phys. **29**, 1621 (1975).
[15] For the Stell-Hemmer potential with a long range attractive tail, the line of first order transitions extends up to the critical point C'. For our 1D short range potential, there cannot exist a critical point for $T > 0$.
[16] S. Sastry, P. Debenedetti, F. Sciortino, and H. E. Stanley, Phys. Rev. E **53**, 6144 (1996).
[17] P. H. Poole, F. Sciortino, U. Essmann, and H. E. Stanley, Nature (London) **360**, 324 (1992); Phys. Rev. E **48**, 3799 (1993); S. Harrington, R. Zhang, P. H. Poole, F. Sciortino, and H. E. Stanley, Phys. Rev. Lett. **78**, 2409 (1997); S. Harrington, P. H. Poole, F. Sciortino, and H. E. Stanley, J. Chem. Phys. **107**, 7443 (1997).
[18] M. P. Allen and D. J. Tildesley, *Computer Simulation of Liquids* (Oxford University Press, New York, 1989).
[19] To each disk we assign a radius $a/2$ in the discrete case, and 0.5 in the smooth case. We define the density ρ to be the ratio of the total area of all the disks to the area of the box. For thermalization we use the Berendsen method of rescaling the kinetic energy [18]. We simulate state points along constant-ρ paths (isochores) [Fig. 2(a)] and also along constant-P paths (isobars). For the isobars, in addition to thermalizing, we achieve a preset P by rescaling the particle positions and the box size every 10^4 time steps ($\delta t = 0.01$), using the value of the virial and its derivative [see J. Q. Broughton *et al.*, J. Chem. Phys. **75**, 5128 (1981)]. We use the isobar results to check the values of $\rho(T, P)$ calculated from isochores, as well as to find K_T along isobars [Fig. 2(b)].
[20] *Ordering in Two Dimensions*, edited by S. K. Sinha (North-Holland, New York, 1980).
[21] When K_T is finite, a minimum along the isochore implies $\alpha_P = 0$, since $(\partial P/\partial T)_V = \alpha_P/K_T$.
[22] This is consistent with the Clausius-Clapeyron equation $dP/dT = \Delta S/\Delta V$, which relates the slope of a first order transition line to the difference between the entropy and volume of the phases. While the solid has a lower entropy, it has a larger volume along the negatively sloped freezing line, and a smaller volume along the positively sloped line.
[23] We calculate K_T using $K_T = \lim_{q\to 0} S(q)/\rho k_B T$, where the structure function $S(q)$ is the Fourier transform of the pair distribution function $g(r)$.
[24] J. E. Lennard-Jones and A. F. Devonshire, Proc. R. Soc. London A **163**, 53 (1937); **165**, 53 (1938); **169**, 53 (1939); **170**, 53 (1939).
[25] We estimate this transition average interparticle distance $\langle r_0 \rangle$ from the location of the minimum between the two subpeaks of the first peak in $g(r)$ [Fig. 3(b)] to be around $r \sim 1.3$ which corresponds to a density $\rho \sim 0.54$ or, at $T = 0.65$, to a pressure $P \sim 1.7$. These estimates are consistent with the location of the maximum D point in Fig. 2(c).